

# Synthesis of Pyrazinoporphyrazine Derivatives Functionalised with Tetrathiafulvalene (TTF) Units: X-Ray Crystal Structures of Two Related TTF Cyclophanes and Two Bis(1,3-dithiole-2-thione) Intermediates

Changsheng Wang, Martin R. Bryce,\* Andrei S. Batsanov and Judith A. K. Howard

*Dedicated to Professor Fabian Gerson on the occasion of his retirement*

**Abstract:** The pyrazinoporphyrazine system **13** (metal-free, zinc and copper derivatives) has been synthesised by tetramerisation of 2,3-dicyanopyrazine monomer unit **10**. The structure of **13a–c** has been established by <sup>1</sup>H NMR spectroscopy, UV/Vis spectrophotometry, MALDI-TOF mass spectrometry, cyclic voltammetry and differential pulse voltammetry. The electrochemical redox behaviour of **13a–c** is strongly solvent dependent. The expected two-stage oxidation of the tetrathiafulvalene (TTF) units

of **13a–c** was observed in a range of solvents; in addition, oxidation and reduction of the pyrazinoporphyrazine core of the metal-free derivative **13a** was detected in benzonitrile. On excitation of **13** in the Q-band region no fluorescence was ob-

served, which is presumably the consequence of intramolecular charge transfer between the TTF moieties and the excited state of the central porphyrazine. Molecular modelling studies on **13a** and **13c** are reported. During the course of this work, the novel TTF macrocycles **11** and **20** were synthesised; their X-ray crystal structures reveal severely bent TTF units, the conformations of which are discussed in detail. The X-ray crystal structures of the bis(1,3-dithiole) systems **15** and **18** have also been determined.

## Keywords

crystal structure · cyclophanes · electrochemistry · porphyrazines · tetrathiafulvalenes

## Introduction

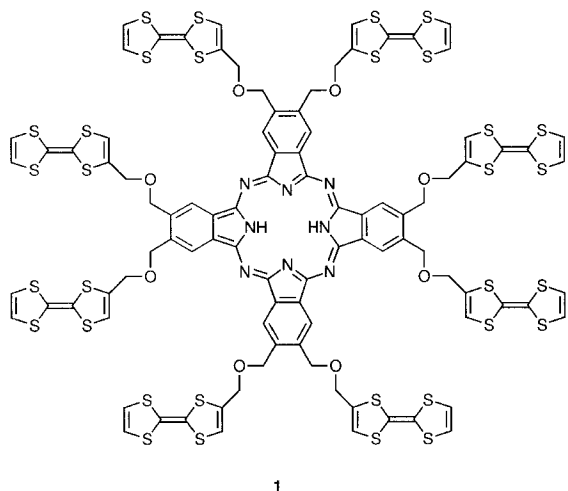
Phthalocyanines and metallophthalocyanines have recently attracted widespread attention in the diverse fields of nonlinear optics, liquid crystals, Langmuir–Blodgett films, electrochromic devices, molecular metals, gas sensors, photosensitisers, and as diagnostic and therapeutic agents in pharmacology.<sup>[1]</sup> These macrocycles display diverse electronic, spectroscopic and structural properties, which can be controlled by metal coordination at the phthalocyanine core and by attachment of peripheral substituents. The most popular synthetic approach, involving cyclotetramerisation of a 1,2-dicyanoarene derivative, produces symmetrical tetra- or octa-functionalised phthalocyanines, and a methodology has also been established for the synthesis of unsymmetrical derivatives.<sup>[2]</sup>

Modifications to the phthalocyanine system include the study of binuclear derivatives,<sup>[3]</sup> heterocyclic analogues<sup>[4]</sup> in which the benzene rings are replaced by nitrogen-containing<sup>[4a–d]</sup> or sulfur-containing heterocycles,<sup>[4e]</sup> and derivatives with specially

designed “active” peripheral substituents, for example, thiolate groups that coordinate transition metals,<sup>[5]</sup> a fullerene moiety that undergoes electrochemical reduction,<sup>[6]</sup> flexible unsymmetrical substituents that result in the formation of glasses,<sup>[7]</sup> mesogenic metal-chelated crown ethers that form nanometer-sized molecular cables,<sup>[8]</sup> and a liquid crystalline ferrocenyl–phthalocyanine system.<sup>[9]</sup>

Tetrathiafulvalene (TTF) is a well-known redox-active compound,<sup>[10]</sup> the derivatives of which have been extensively studied during the last twenty-five years, mainly in the search for new molecular conductors and superconductors.<sup>[11]</sup> The potential of TTF within the wider context of supramolecular chemistry is now recognised and new, more elaborate TTF and multi-TTF systems have been assembled.<sup>[12]</sup> In this context, we have recently reported the synthesis, spectroscopic characterisation and solution redox chemistry of the metal-free **1**, which is the first phthalocyanine derivative bearing tetrathiafulvalene (TTF) substituents.<sup>[13]</sup> Further studies on **1** were hampered by its insolubility in almost all organic solvents. The motivation behind the present work was to combine TTF chemistry and macrocyclic chemistry to obtain novel systems with unusual electrochemical and structural properties. We now describe, for the first time, the synthesis, characterisation and electrochemical study of new, soluble macromolecules of this genre, comprising eight TTF units attached symmetrically to the periphery of the pyrazinoporphyrazine core. We also report here the X-ray crys-

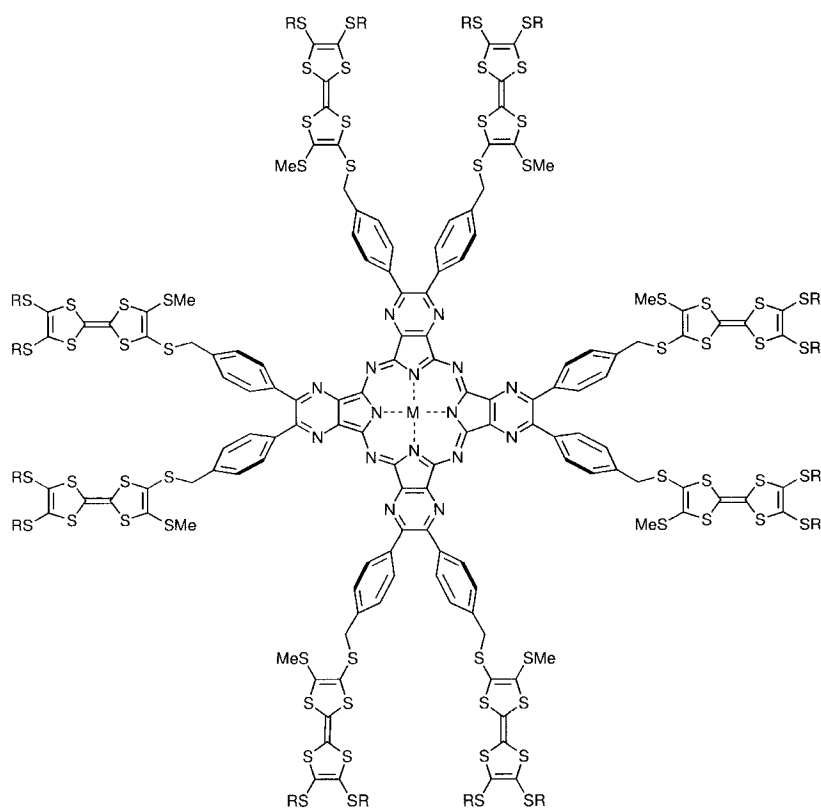
[\*] Dr. C. S. Wang, Professor M. R. Bryce, Dr. A. S. Batsanov, Professor J. A. K. Howard  
Department of Chemistry, University of Durham,  
Durham, DH1 3LE (UK)  
Telefax: Int code +(191)384-4737  
e-mail: m.r.bryce@durham.ac.uk



tal structures of two unusual TTF macrocycles obtained by intramolecular coupling, and the structures of two bis(1,3-dithiole-2-thione) precursors synthesised during the course of this work.

## Results and Discussion

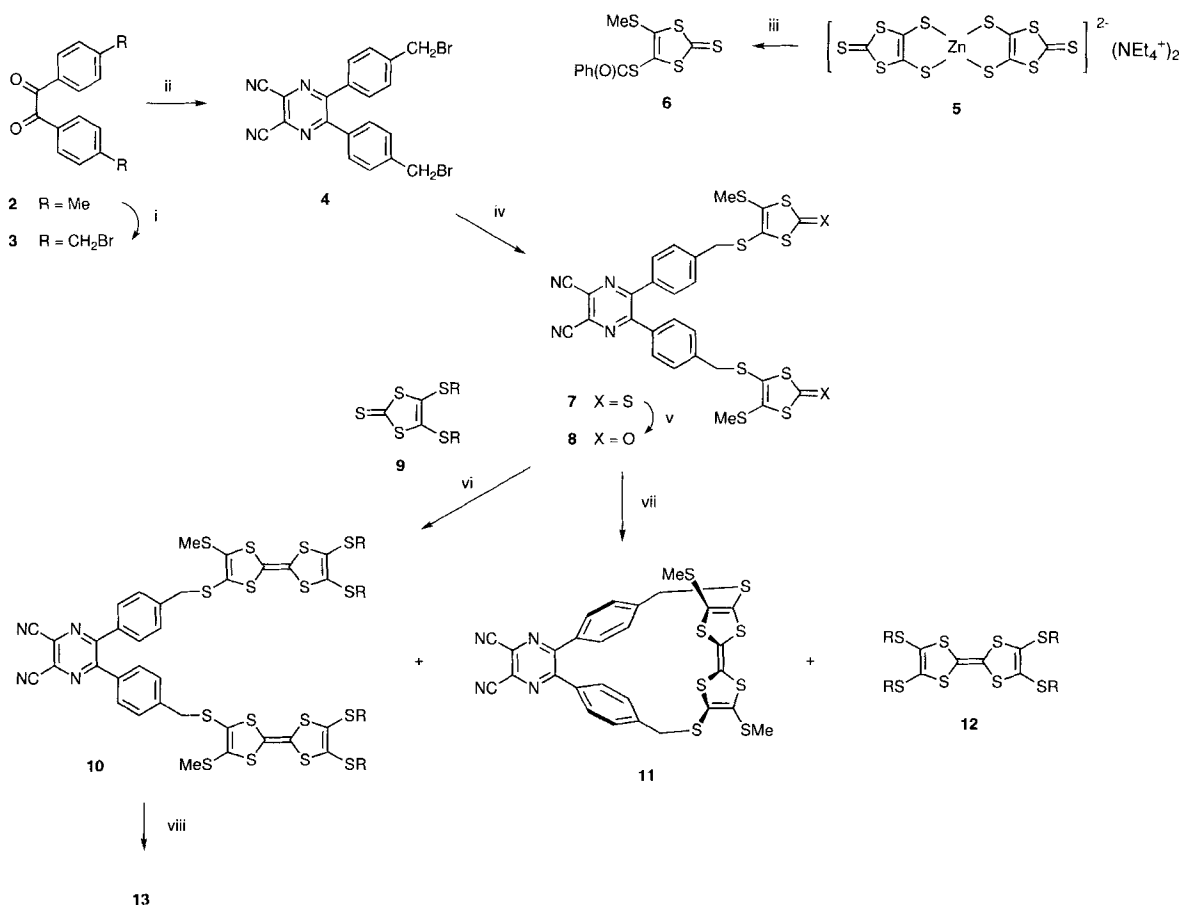
**Synthesis of Pyrazinoporphyrazine Derivatives 13:** Our prime target at the outset of this work was **13**, containing a central pyrazinoporphyrazine core, which we chose for synthetic reasons. In our previous work<sup>[13]</sup> the relatively harsh conditions



**13** a M = H<sub>2</sub>; R = *n*-hexyl  
 b M = Zn; R = *n*-hexyl  
 c M = Cu; R = *n*-hexyl

needed for the formation of the phthalonitrile precursor of **1**, from the corresponding dibromobenzene derivative (CuCN, DMF at 140 °C, 48 h), was found to be problematical in larger-scale reactions, sometimes leading to product mixtures involving decomposition of the appended TTF groups.<sup>[13b]</sup> Therefore, we sought a route that would avoid an arylbromide → arylcyanide conversion in the presence of a TTF unit. The key features of our synthetic strategy (Scheme 1) are as follows: 1) 1,2-dicyanopyrazine derivatives are easily prepared from diaminomaleonitrile and 1,2-diketones, and there are precedents for their cyclotramerisation to yield pyrazinoporphyrazines;<sup>[4c, d]</sup> 2) solubility may be achieved by virtue of the extra nitrogen atoms and the peripheral alkyl chains, which can be introduced by using the readily available 4,5-bis(alkylthio)-1,3-dithiole-2-thione unit **9**<sup>[14]</sup> in the synthesis of the TTF fragments; 3) the methodology should be versatile with respect to both the peripheral alkyl substituents and the linking group between the pyrazine and TTF systems.

Pyrazine derivative **4** was readily synthesised starting from 4,4'-dimethylbenzil (**2**). Bromination to yield **3** (71% yield) was followed by reaction with diaminomaleonitrile in acetic acid to yield **4** (67% yield). Reaction of **4** with two equivalents of the thiolate anion liberated on treatment of **6** with sodium methoxide<sup>[15]</sup> afforded the bis(1,3-dithiole-2-thione) system **7** (52% yield). Dithione **7** was then converted into the corresponding diketone **8** (80% yield) by a standard reaction with mercury(II) acetate in acetic acid. Reaction of diketone **8** with 4,5-bis(hexylthio)-1,3-dithiole-2-thione (**9**)<sup>[14]</sup> in the presence of triethylphosphite afforded three products that were separated by column chromatography. The major product was the cross-coupled bis(TTF) derivative **10** (35% yield). The other two products were identified as macrocycle **11** (25% yield), obtained by the intramolecular coupling of the ketone groups of **8** (an X-ray structural analysis confirmed the “*trans*” structure of **11**, see below) and tetrakis(hexylthio)-TTF (**12**), obtained by self-coupling of **9** (9% yield). Another possible product, the bis(TTF) derivative, which could conceivably be formed by intermolecular coupling<sup>[16]</sup> of **8**, was not isolated from the reaction mixture. The yield of **11** was raised to 51% by heating **8** in the presence of triethylphosphite. The “*cis*” isomer of **11** was not detected based on chromatography and the X-ray diffraction patterns of different crystals grown by fractional recrystallisation from different solvents. It is noteworthy that the <sup>1</sup>H NMR spectrum of **11** suggests a rigid structure in solution at room temperature. The four benzylic protons of **11** are split into two doublets of equal intensity at  $\delta = 4.21$  and 3.80, each displaying a geminal coupling constant of 13 Hz, whereas in **7**, **8**, and **10** these four protons are identical, giving rise to a singlet at  $\delta = 4.03$ , 4.02, and 3.98, respectively. Compound **10** underwent cyclotramerisation in the presence of lithium pentoxide in a mixture of pentanol and dioxane as solvent<sup>[17]</sup> at ca. 125 °C for 30–45 min; treatment with acetic



Scheme 1. i) *N*-bromosuccinimide, benzoyl peroxide, hv, CCl<sub>4</sub>, reflux; ii) diaminomaleonitrile, AcOH, reflux; iii) benzoyl chloride, methyl iodide, acetone, 20 °C; iv) 6. NaOMe, MeOH, 40 °C; v) Hg(OAc)<sub>2</sub>, CHCl<sub>3</sub>, AcOH, 20 °C; vi) 9, P(OEt)<sub>3</sub>, 115 °C; vii) P(OEt)<sub>3</sub>, 115 °C; viii) LiOPh, PhOH/1,4-dioxane, 125 °C, then AcOH (for **13a**), Zn(OAc)<sub>2</sub> for **13b**, CuCl<sub>2</sub> (for **13c**). R = *n*-hexyl.

acid afforded the metal-free system **13a** in 64% yield. Addition of zinc acetate or copper(II) chloride to a solution of the crude product in chloroform afforded the zinc and copper pyrazinoporphyrazine derivatives **13b** (45% yield) and **13c** (31% yield), respectively, whereas heating for longer than 2 h led to black, insoluble products, indicating decomposition of the dinitriles or the macrocycles. Compounds **13a–c** are air-stable, dark-green solids, which were purified by stepwise extraction. Attempts at purification by column chromatography on both silica and alumina were unsuccessful: decomposition or oxidation seemed to occur. Structures **13a–c** were assigned on the basis of elemental analysis, MALDI-TOF mass spectra and UV/Vis spectra, which were all entirely consistent with the pyrazinoporphyrazine structure. <sup>1</sup>H NMR spectra at 20 °C in a range of solvents gave broad lines at the expected chemical shifts, with little fine structure. (The spectrum of the copper derivative **13c** was further broadened by paramagnetic effects.) The UV/Vis spectra of metal-coordinated derivatives **13b** and **13c** in dichloromethane showed a single Q-band absorption at  $\lambda_{\max} = 664$  (**13b**) and 659 nm (**13c**), which was more intense for the copper derivative. On addition of excess iodine to the solution a new, broad, low-energy absorption band emerged at  $\lambda_{\max} = 815$  (**13b**) and 835 nm (**13c**) which were clearly observed in the subtraction spectra, consistent with the formation of tetrathiafulvalenyl cation radicals<sup>[18]</sup> (the new band at 500 nm is ascribed to excess molecular iodine) (Figure 1 for **13c**). The

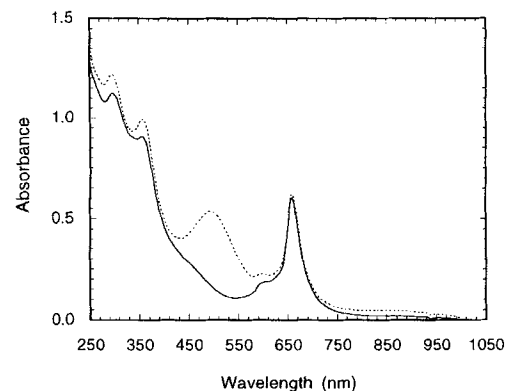


Figure 1. UV/Vis spectra of **13c** in DCM at 20 °C before (solid line) and after (dotted line) addition of iodine.

UV/Vis spectrum of **13a** in dichloromethane, chloroform, benzene, toluene, pyridine, carbon disulfide, *o*-dichlorobenzene and chloroform/acetic acid mixture gave a single Q-band at  $\lambda_{\max} \approx 665$  nm; in a mixture of *o*-dichlorobenzene/acetic acid (1:1 v/v) the characteristic split Q-band of a metal-free phthalocyanine was observed with absorptions at  $\lambda_{\max} = 654$  and 676 nm. Significant solvent effects on both the extinction coefficient and the shape of the Q-bands of **13a–c** were observed.

On excitation of **13** over a range of concentrations in toluene in the Q-band region no fluorescence was observed, which sug-

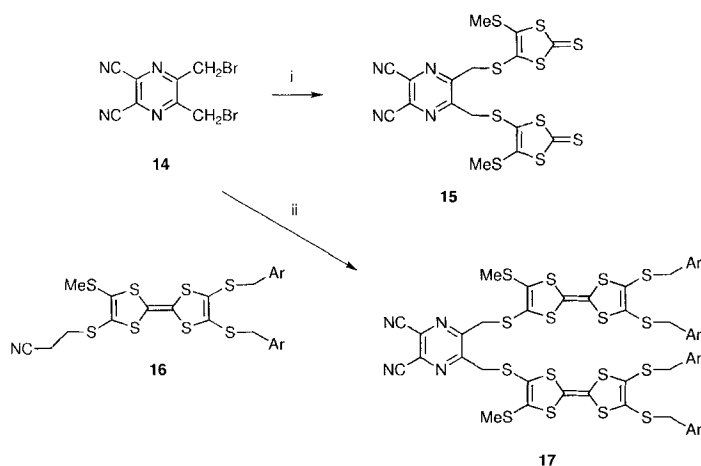
gests that a very efficient quenching process is occurring. This is presumably the consequence of intramolecular charge transfer between the TTF moieties and the excited state of the central porphyrazine<sup>[19]</sup> totally quenching its energy emission relaxation. In support of this claim, the quenching of the fluorescence of tetrabutyl-(H<sub>2</sub>)Pc by TTF was studied, and a diffusion-controlled charge-transfer process was observed, with  $k_Q = 1.1 \pm 0.1 \times 10^{10} \text{ mol}^{-1} \text{ dm}^3 \text{ s}^{-1}$ . The results of this study along with the photophysical properties of new covalently tethered (TTF)<sub>8</sub>-Pc systems, in which there is intramolecular electron transfer between the Pc core and peripheral TTF, will be reported in due course.<sup>[20]</sup>

**Extension to the Related TTF Macrocycles 20 and 21:** Although **13a–c** are quite soluble in many organic solvents (e.g., carbon disulfide, dichloromethane, chloroform) our attempts to crystallise them for X-ray analysis have proved unsuccessful, and amorphous solids were always obtained. We believe that the phenylene spacers between the central macrocycle and the TTF moieties in **13** allow considerable free rotation of the peripheral TTF groups, leading to disorder of the molecules in the solid state. We hoped, therefore, that pyrazine derivative **17**, with the phenylene spacers removed, would lead to a pyrazinoporpyrazine analogue of **13** possessing a more ordered solid state structure that could be easier to crystallise. In addition, there is considerable current interest in the incorporation of TTF units into macrocyclic frameworks,<sup>[12a, 21, 22]</sup> and in the light of the facile formation of **11**, we considered that it was timely to explore this reaction further. Compound **15** was synthesised by reaction of pyrazine derivative **14** with two equivalents of the sodium thiolate salt of **6** (90% yield, Scheme 2). However, heat-

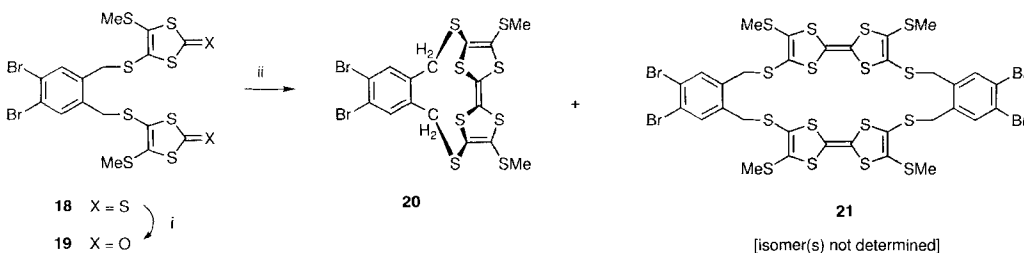
ing **15** in triethylphosphite at 125 °C failed to yield any isolable products, possibly due to the low solubility of **15** under these conditions. Elevated temperature resulted in decomposition of **15** or its derived products. Compound **15** could not be converted into the corresponding diketone under the same conditions that allowed conversion of **7** into **8**, again due to low solubility.

In an attempt to circumvent this problem we deprotected compound **16**<sup>[23]</sup> (2 equiv) by reaction with caesium hydroxide, and the derived thiolate anion was allowed to react with **14** to yield the expected bis(TTF) derivative **17** (79% yield). However, **17** was unstable to the strongly basic conditions needed for pyrazinoporpyrazine formation, probably because the strongly electron-withdrawing dicyanopyrazine group makes the adjacent methylene protons very acidic, and deprotonation or C–S bond cleavage occurs at this site. The related *o*-benzene derivative **18** was prepared from the corresponding bis(bromomethyl)benzene derivative and the sodium thiolate salt of **6** in 82% yield, and converted into the diketone analogue **19** (89% yield) (Scheme 3). Heating **19** in triethylphosphite at 125 °C afforded **20** and **21** (combined yield 87%) in a ratio of ca. 2:1, formed by intramolecular and intermolecular coupling,<sup>[16]</sup> respectively. The isomer ratio was assigned from the integration of the benzylic protons in the <sup>1</sup>H NMR spectrum. In cyclophane **20** these protons are split into two singlets of equal intensity at  $\delta = 4.18$  and 3.47 ( $J = 16 \text{ Hz}$ ) (which is similar to that of **11**), while in **21** these protons are observed as a singlet at  $\delta = 4.09$ .

The X-ray crystal structures of **15** (Figure 2), **18** (Figure 3), **11** and **20** were determined (see below).



Scheme 2. i) **6**, NaOMe, MeOH, 40 °C; ii) **16**, CsOH·H<sub>2</sub>O, DMF, 20 °C. Ar = 4-Me-C<sub>6</sub>H<sub>4</sub>.



Scheme 3. i) Hg(OAc)<sub>2</sub>, CHCl<sub>3</sub>, AcOH, 20 °C; ii) P(OEt)<sub>3</sub>, 125 °C.

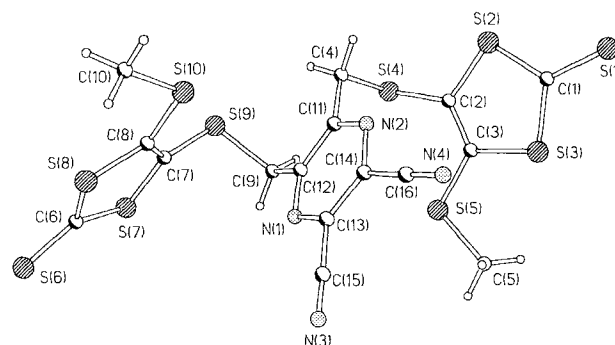


Figure 2. X-Ray molecular structure of **15**.

**Solution Electrochemical Studies:** The solution electrochemistry of representative new TTF derivatives synthesised in this work was studied by cyclic voltammetry (CV) (Table 1). Compound **10** shows the expected two reversible oxidation waves in both dichloromethane and in dimethylformamide, at potentials typical of a tetrakis(alkylthio)TTF derivative (thioalkyl substitution

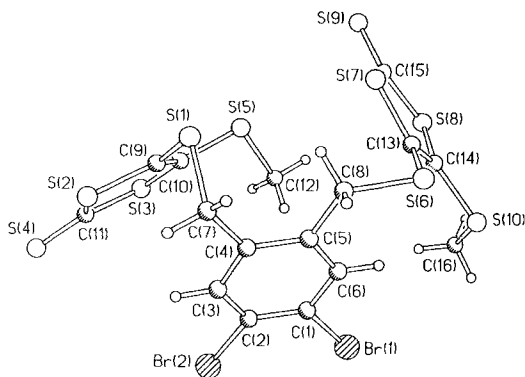
Figure 3. X-Ray molecular structure of **18**.

Table 1. Cyclic voltammetric data [a].

	Solvent	$E_1^{\text{ox}}$	$E_1^{\text{rev}}$	$E_2^{\text{ox}}$	$E_2^{\text{rev}}$
<b>10</b>	DCM	0.61	0.52	0.87	0.77
	DMF	0.72	0.65	0.88	0.80
	DCM/DMF [b]	0.72 [d]	0.63	0.90	0.82
<b>11</b>	DCM	0.70	0.52	0.82	0.73
	DMF	0.83	0.77		0.63
<b>13a</b>	DCM	0.62	0.51	0.89	0.76
	DMF	0.71	0.63	0.88	0.81
	benzonitrile [c]	0.63	0.47	0.95	0.81
	DCM/DMF [b]	0.68	0.59	0.89	0.80
<b>13b</b>	DCM	0.59	0.50	0.88	0.74
	DMF	0.72	0.66	0.90	0.83
	benzonitrile	0.63	0.50	0.96	0.81
	DCM/DMF [b]	0.71	0.61	0.94	0.81
<b>13c</b>	DCM	0.58	0.53	0.86	0.73
	DMF	0.62	0.31	0.73	
	benzonitrile	0.65	0.57	0.79 [d]	0.83
	DCM/DMF [b]	0.45	0.34		0.63
<b>17</b>	DCM	0.71	0.60	1.02	0.93
	DMF	0.75	0.64	0.93	0.83
	benzonitrile	0.71	0.61	1.00	0.92
<b>20</b>	DMF	1.24			
<b>21</b>	DMF	0.73	0.65	0.91	0.83

[a] Working and counter electrodes: Pt; reference electrode: Ag/AgCl; supporting electrolytes:  $\text{Bu}_4\text{NClO}_4$  (0.1 M); scan rate:  $100 \text{ mVsec}^{-1}$ . [b] 1:1 (v/v). [c] Additional wave observed at  $E_3^{\text{ox}} = 1.22$  and  $E_3^{\text{rev}} = 1.18$  V. [d] Detected by DPV; for conditions, see Figure 4b.

is known to raise the oxidation potential, relative to TTF itself,<sup>[24, 25]</sup> and solvent effects on TTF peak potentials are well documented).<sup>[24]</sup> As expected, the TTF units in **10** do not appear to interact. It has been shown in previous CV studies on bis(TTF) derivatives linked by a variety of spacer groups<sup>[26]</sup> that there is usually no observable interaction between the TTF ring systems unless they are linked by a single-atom spacer<sup>[27]</sup> or are directly attached.<sup>[28]</sup> The cyclic voltammogram of cyclophane **11** is strongly solvent-dependent: in dichloromethane two ill-resolved redox waves are observed on the oxidative scan at peak potentials of 0.70 and 0.82 V. In DMF, however, the two waves totally overlap at a peak potential of 0.83 V. The latter is presumably a two-electron wave, as two distinct waves are observed at peak potentials of 0.77 and 0.63 V on the reverse reductive scan (Table 1). The cyclic voltammogram of the strained cyclophane **20** is markedly different from that of the less-distorted structure **11**. For **20** a single irreversible oxidation

at  $E^{\text{ox}} = 1.24$  V occurs in DMF. This is consistent with CV data reported by Becher et al. for other severely bent TTF derivatives; this indicates that significant deviation from planarity of the TTF system destroys its donor ability by preventing efficient  $6\pi$ -electron delocalisation (heteroaromaticity) within the dithiolium cation structure formed on oxidation.<sup>[22d]</sup> In spite of its low solubility, the macrocycle **21** exhibits two cleanly reversible oxidation waves in DMF, consistent with planar (or near-planar) TTF units.

The electrochemical oxidation of pyrazinoporphyrazine derivatives **13a–c** was studied in a range of solvents and strong solvent dependency was observed; representative data are included in Table 1. In dichloromethane, all three compounds **13a–c** displayed the two TTF redox waves at oxidation potentials similar to those of the building block **10**, which were reversible at a scan speed of  $100 \text{ mVs}^{-1}$ . Although the two redox couples of the Zn derivative **13b** appeared to be reversible, the intensity of the second couple was smaller than that of the first, which might suggest incomplete second oxidation of the TTF units. No other significant reduction or oxidation of the core pyrazinoporphyrazine was observed for **13a–c** in dichloromethane. Use of DMF, which is not a good solvent for this class of compound, led to a considerable distortion in the cyclic voltammograms of **13a–c**: the reversibility of the two-stage oxidation decreased with decreasing solubility along the sequence **13a** > **13b** > **13c**. For the Cu derivative **13c**, the two oxidation peaks appeared much closer together ( $\Delta E^{\text{ox}} = 110$  mV) compared with those in DCM ( $\Delta E^{\text{ox}} = 280$  mV), and the reductive peaks in the reverse scan overlapped into one peak, which shifted to a lower potential (0.31 V). Again, no reduction or oxidation peaks of the macrocyclic core were observable for **13a–c** in DMF. The use of a mixture of DCM and DMF as solvent improved the reversibility of the electrochemical response of **13a** and **13b**, but had no effect on **13c**. The two-wave oxidation of **13a** and **13b** in this solvent mixture was nearly reversible, although the intensity of the second couple was considerably lower than that of the first at high scan rates ( $500 \text{ mVs}^{-1}$ ) (Table 1). At slow scan rates ( $10 \text{ mVs}^{-1}$ ) the two peaks were of comparable intensity, but the corresponding second reductive peak in the reverse scan remained unchanged. This effect of differing scan rates (increased intensity of the second oxidation at slow scan speed) is indicative of relative motion of the TTF moieties in the molecules on the voltammetric time-scale. The cyclic voltammograms of **13a–c** in benzonitrile were different. The two-stage oxidative peaks of the Cu derivative **13c** on the forward anodic scan overlapped into one broad peak in benzonitrile at  $E^{\text{ox}} = 0.65$  V (with a shoulder at 0.79 V detected by differential pulse voltammetry (DPV)). However, the two cathodic reductive peaks on the reverse scan were unchanged at 0.57 and 0.83 V. For the Zn derivative **13b** in benzonitrile, a broadening of the second oxidative peak was observed at a potential corresponding to the oxidation of pyrazinoporphyrazine core of **13a** (Figure 4a), although no corresponding cathodic response was seen on the reverse scan. Cyclic voltammetry of **13a** in benzonitrile (Figure 4a) showed, in addition to the two TTF waves, a third wave at  $E_3^{\text{ox}} = 1.24$  and  $E_3^{\text{red}} = 1.18$  V, which was not observed for the metallo-derivatives **13b** and **13c**. We assign this wave to a single-electron oxidation of the pyrazinoporphyrazine core unit. The DPV of

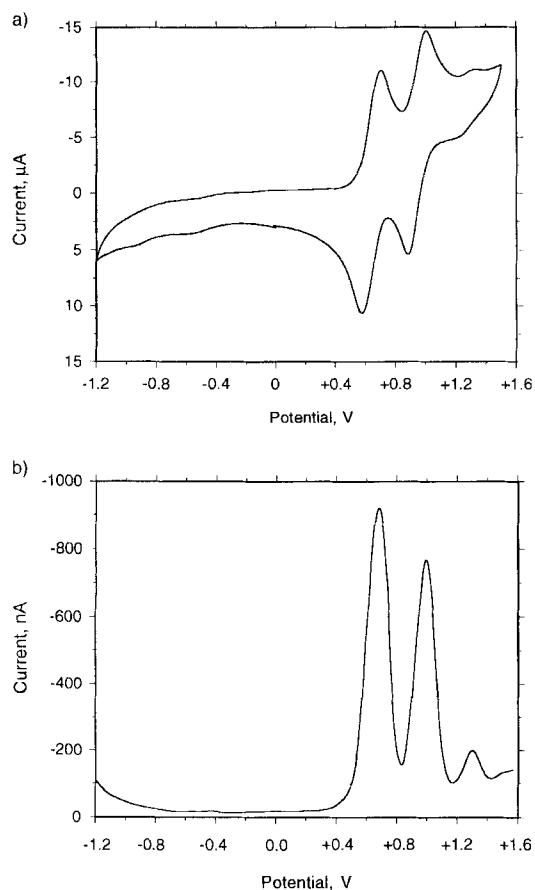


Figure 4. a) Cyclic voltammogram (the conditions are reported in Table 1) and b) differential pulse voltammogram of **13a** in benzonitrile. Experimental conditions: scan rate  $50 \text{ mVs}^{-1}$ ; sample width 10 ms; pulse amplitude 50 mV; pulse width 20 ms; pulse period 100 ms; for electrodes see Table 1.

**13a** (Figure 4b) shows this wave clearly and, based on the current passed for the DPV peaks, we suggest that all the TTF units are oxidised, although it is noteworthy that the two TTF waves are not of equal intensity, possibly due to adsorption phenomena or instability of the fully oxidised TTF units. It is apparent, therefore, that the electrochemical behaviour of compounds **13a–c** is dependent not only on the molecular structure but also on the solvent: the latter will effect the conformation, the extent of aggregation and the rate of diffusion.

Estimating accurately the number of electrons transferred in multi-redox waves is a common problem with redox-active dendrimers and hyperbranched systems, because of the slower diffusion rates of the dendrimer compared with an internal reference compound.<sup>[29]</sup> The two different redox functionalities within the macromolecule **13a**, which are oxidised at significantly different potentials, provide a convenient covalently bound internal reference. Similar data have been obtained for other dendrimers that contain different redox units (e.g., metal-bipyridyl and ferrocene derivatives).<sup>[30]</sup>

Extensive studies on the cathodic electrochemistry of phthalocyanines have been reviewed recently,<sup>[31]</sup> but very little electrochemical data are available on pyrazinoporphyrazines, although it has been reported that the reduction of Zn-pyrazinoporphyrazine derivatives occurs at a potential that is 0.44 V more positive than that of the corresponding

Zn-phthalocyanine.<sup>[4b]</sup> In general, no clear reduction wave was observed for **13b** or **13c** in any of the solvents mentioned above. However, for the metal-free system **13a** in benzonitrile a very shallow reversible redox couple was observed at ca.  $-0.45 \text{ V}$  (Figure 4a,b), which we tentatively assign to the reduction of the pyrazinoporphyrazine core. We note that the intensity of this wave, compared with the oxidation process, is too weak for a one-electron reduction. However, in other work on a related phthalocyanine system, the intensity of the reduction wave was found to be solvent-dependent.<sup>[20]</sup>

**Molecular Modelling Studies of 13a and 13c:** Molecular modelling of **13a** and **13c** was performed. We first found the energetically most favourable conformer of subunit **10** to provide an appropriate conformation for use in the minimisation of the structure of **13a** and **13c**. A folded conformation with  $C_2$  symmetry gave the lowest energy structure for **10** (Figure 5). Based

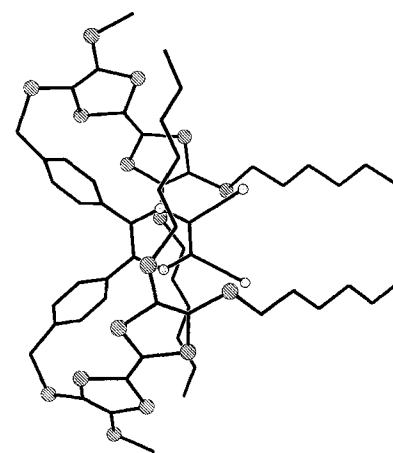


Figure 5. Energy-minimised conformation of **10**.

on this conformation, we minimised the structure of **13c**, using four fragments with similar TTF orientations, to give a folded structure possessing two pairs of TTF units on each side of the mean macrocycle plane. It is worth noting that the total molecular energy for **13c** decreased with increasing folding of the TTF units, suggesting that there may be a decrease in molecular energy resulting from interactions between the TTF units and the central metallomacrocycle. If the molecules of **13c** adopt a similar conformation in solution<sup>[32]</sup> to the computer-optimised structure, the metallopyrazinoporphyrazine core will be extensively shielded by the TTF units and their attached alkyl chains: this could be an important factor in modulating the electrochemical properties of the core of the molecule, the oxidation of which was not observed in the cyclic voltammogram (see above). The energy-minimised conformation of metal-free derivative **13a** (Figure 6a) was similarly folded to **13c**. However, for **13a**, a partially open conformation (Figures 6b and 6c) was attainable at an energy only  $34 \text{ kcal mol}^{-1}$  higher than that of the folded conformation, whereas for **13c** the next energy valley was  $112 \text{ kcal mol}^{-1}$  above the energy-minimised conformation. This difference between **13a** and **13c** could be due to metal chelation in the latter compound limiting the flexibility of the porphyrazine macrocycle. We suggest that a partially open

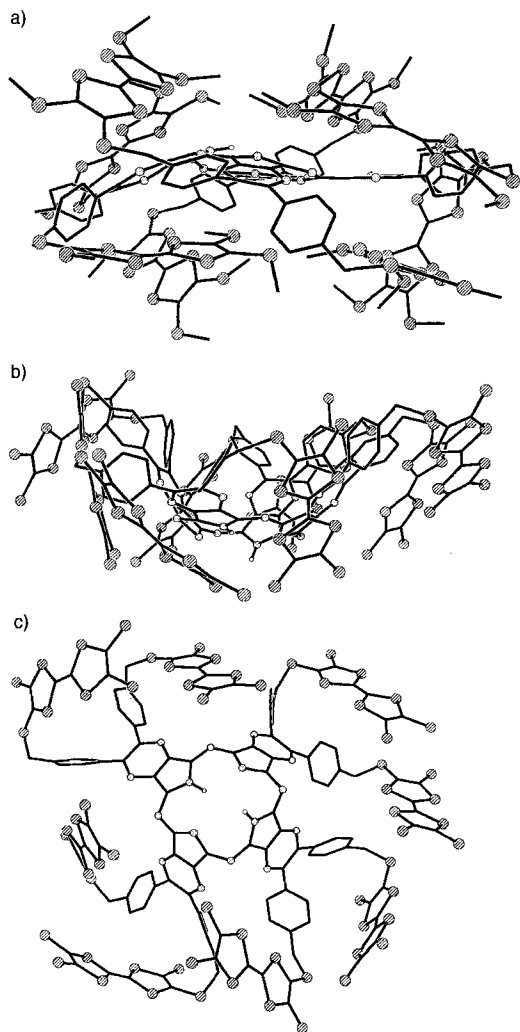


Figure 6. a) Energy-minimised conformation of **13a** (the alkyl chains are omitted for clarity); b) The partially open conformation of **13a**, which is  $34 \text{ kcal mol}^{-1}$  higher in energy than the closed conformation shown in Figure 6a, viewed side-on to the pyrazinoporphyrazine ring; c) As Figure 6b, top view onto the pyrazinoporphyrazine ring.

conformation, similar to those shown in Figures 6a and b, is accessible to **13a** in solution (but not for **13c**), thereby enabling the redox chemistry of the pyrazinoporphyrazine core of **13a** to be observed. We note that Diederich, Gross and co-workers have recently demonstrated that the redox properties of dendritic porphyrins can be modulated by steric shielding of the porphyrin core.<sup>[33]</sup>

**X-Ray Crystal Structures of 11 and 20:** The structures of **11** and **20** are of special interest because of the severe bending of their TTF moieties, which are incorporated into macrocycles, that is, the dithiole rings are bridged in a *trans* fashion in **11** and in a *cis* fashion in **20**. Notwithstanding the popularity of the TTF moiety,<sup>[11, 12a]</sup> its conformation has never been studied systematically. The planarity of this highly  $\pi$ -conjugated system is usually taken for granted,<sup>[34]</sup> with statements like “TTF is a rigid molecule and large variations in the features are not expected”.<sup>[34c]</sup> In fact, TTF can display substantial nonplanarity, which can be described by five angles (Figure 7), namely, 1)  $\theta_1$  and  $\theta_2$  (folding of each dithiole ring along the  $\text{S} \cdots \text{S}$  vectors), 2)  $\phi_1$  and  $\phi_2$

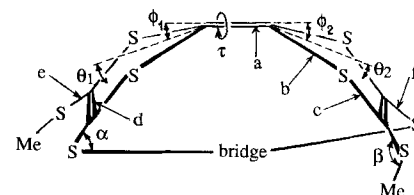


Figure 7. Geometric features of the TTF moiety.

(inclinations of the central  $\text{C}=\text{C}$  bond to each adjacent  $\text{CS}_2$  plane) and 3)  $\tau$  (average  $\text{S}-\text{C}-\text{C}-\text{S}$  torsion angle around the central  $\text{C}=\text{C}$  bond). Most common is type 1 bending in a boat (rarely chair) fashion, with the central  $\text{C}_2\text{S}_4$  system remaining planar ( $\phi_1, \phi_2, \tau \approx 0$ ). Distortions of type 2 and 3 occur rarely and only in the most sterically constrained systems.

It is noteworthy that although unsubstituted TTF is planar in both its crystal polymorphs,<sup>[34b, c]</sup> this is not the case in the gas phase; electron diffraction studies<sup>[35]</sup> indicate a boat conformation with  $\theta_{1,2} = 13.5^\circ$ . Substituted TTF derivatives (including BEDT-TTF) often adopt much bigger bending:  $\theta$  exceeds  $13^\circ$  in 45 neutral molecules (besides five CT complexes and 13 salts with partially oxidised TTF derivatives),<sup>[36]</sup> in 11 of which the TTF moiety is incorporated into macrocyclic frameworks.<sup>[21, 22]</sup> The shortest bridges known (seven-membered), in **22**,<sup>[22b, d]</sup> enforce a  $\theta$  angle of  $36\text{--}43^\circ$  and a  $\phi$  angle of  $7\text{--}17^\circ$ , while  $[\text{S}(\text{CH}_2)_n\text{S}]$  bridges with  $n = 10$  and  $12$  leave TTF essentially planar.<sup>[22e]</sup>

However, the rest of the “bent” TTF derivatives are free from such constraints, and the bending must be attributed entirely to electronic effects, namely, the coupling between TTF HOMOs and their consequent splitting into a bonding  $\text{HOMO}_+$  and antibonding  $\text{HOMO}_-$ . (Packing itself is unlikely to cause bending, as planar species can usually pack more densely than those that are bent. A peculiar exception is  $\text{C}_{60} \cdot 2(\text{BEDT-TTF})$ , in which boat-shaped TTF moieties ( $\theta_1 = 23$  and  $\theta_2 = 32^\circ$ ) are “wrapped” around a spherical fullerene molecule.<sup>[37]</sup>)

The TTF HOMO is heavily localised on the central  $\text{C}_2\text{S}_4$  moiety;<sup>[27b, 34d]</sup> thus, folding of the dithiole rings enhances the localisation still further and lowers its orbital energy.<sup>[22d, 27b]</sup> In agreement with this description, oxidation potentials of strongly bent (bridged) TTF derivatives are relatively high, although no clear correlation between bending and  $E_{\text{ox}}$  was found.<sup>[22d]</sup> Any coupling of HOMOs might be intra- or intermolecular. The intramolecular interaction can occur between two TTF moieties linked through a direct covalent bond or a conducting bridge, as in TTF-Te-Te-TTF,<sup>[27b]</sup> where one TTF moiety is planar and another is bent with  $\theta_1 = 13^\circ$  and  $\theta_2 = 19^\circ$ , the  $\text{HOMO}_-$  supposedly being localised on the former and the  $\text{HOMO}_+$  on the latter. Bis-TTF-1,4-ditellurines (with two Te bridges between TTF moieties) exhibit the largest  $\theta$  values among nonmacrocyclic TTF derivatives ( $30\text{--}33^\circ$ ).<sup>[38]</sup> More widespread intermolecular coupling is usually associated with molecular dimers, that is, two TTF systems contacting face-to-face, adopting boat conformations with the central planar  $\text{C}_2\text{S}_4$  moieties overlapping usually in a ring-over-bond fashion (i.e., dithiole over the central  $\text{C}=\text{C}$  bond) and the peripheral parts bending outwards.<sup>[39]</sup> The parallel slip of ca.  $1.6 \text{ \AA}$  between the molecules minimises the  $\text{S} \cdots \text{S}$  repulsion. Earlier semiempirical<sup>[34d]</sup> and molecular mechanical<sup>[34e]</sup> calculations of the  $(\text{TTF})_2$  dimer

could give this pattern of overlap, but all of them *presupposed* molecular planarity, reasoning from the crystal structure of (monoclinic) TTF.<sup>[34b]</sup> The motif of the latter, however, is a uniform infinite stack rather than separate dimers. More recent ab initio calculations for the [TTF–C(O)NMe<sub>2</sub>]<sub>2</sub> dimer with full relaxation of molecular geometry reproduced the folding pattern correctly.<sup>[39b]</sup> However, this easily recognisable (and explainable) packing is not the only one known; for example, in the monoclinic polymorph of tetra(methylthio)TTF (average  $\theta = 25^\circ$ ) molecules contact perpendicularly, face-to-edge.<sup>[40]</sup> Planarity of the same molecule in the triclinic modification<sup>[41]</sup> is a good illustration of the flexibility of TTF. Ab initio 6-31G\* calculations for an isolated TTF molecule<sup>[39b]</sup> confirm its high flexibility and although the potential minimum does correspond to a planar conformation, the energy cost of folding both dithiole rings to  $\theta = 5^\circ$  is practically zero (0.016 kcal mol<sup>-1</sup>) and those for  $\theta = 10, 15$  and  $20^\circ$  are also relatively small (0.1, 0.4 and 1.0 kcal mol<sup>-1</sup>, respectively).

The present structures can be instructive on the limits of TTF deformations (especially as the six-membered bridge linking the dithiole rings in **20** is the shortest known) and also whether a bridge-induced TTF bending can bring about an especially strong dimeric interaction.

The X-ray structure of **11** was determined in both monoclinic (**11a**) and triclinic (**11b**) forms, obtained from CS<sub>2</sub> and CH<sub>2</sub>Cl<sub>2</sub>, respectively. The asymmetric unit of **11a** comprises one molecule of **11** (Figure 8) and one (partially disordered) of CS<sub>2</sub>, while that of **11b** comprises two molecules of **11** (A and B, see Figure 9) and two of CH<sub>2</sub>Cl<sub>2</sub> (one of which is disordered). All three molecules of **11** have essentially the same geometry (see Table 2). The  $\theta$  folding along the S(1)⋯S(2) and S(3)⋯S(4) vectors is 28.2 and 30.4 (**11a**), 25.9 and 29.5 (**11b**, molecule A),

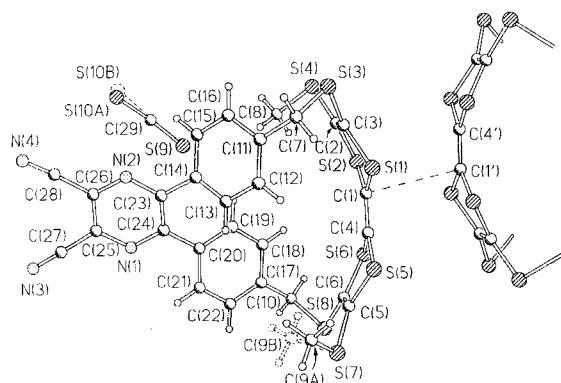


Figure 8. Molecules **11** and CS<sub>2</sub> in the structure of **11a**, showing the disorder (dashed) and short contacts with an inversion-related molecule (primed atoms).

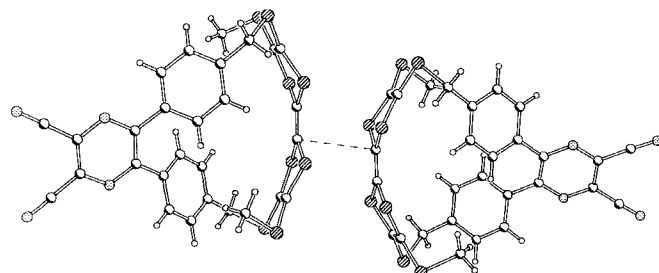


Figure 9. Two independent molecules of **11** in **11**·CH<sub>2</sub>Cl<sub>2</sub> (**11b**); atomic numbering is identical with **11a**.

Table 2. Selected average geometric parameters (distances, Å; angles, °) of **11** and **20** [a].

	<b>11a</b>	<b>11b</b>	<b>20</b>
<i>a</i>	1.348 (7)	1.343 (6)	1.347 (13)
<i>b</i>	1.751 (5)	1.759 (4)	1.763 (8)
<i>c</i>	1.770 (5)	1.770 (4)	1.773 (7)
<i>d</i>	1.335 (7)	1.347 (6)	1.359 (9)
<i>e</i>	1.743 (5)	1.750 (4)	1.745 (7)
<i>f</i>	1.749 (5)	1.753 (4)	1.750 (7)
$\alpha$	100.8 (2) [b]	100.2 (2)	103.4 (4)
$\beta$	101.3 (2)	100.3 (2)	98.7 (3)
$\theta$	29	29	41.6
$\phi$	1.0	1.0	12.7
$\tau$	3.9	1.7	0

[a] Notation, see Figure 7; [b] For ordered C atoms.

27.7 and 31.5° (**11b**, molecule B), respectively;  $\tau$  torsion is small (1.4–3.9°) and  $\phi$  tilting is negligible (0.1–1.6°). The steric strain elsewhere in the macrocycle seems rather small for such a rigid system. Thus, bond angles at the macrocyclic S(3) and S(8) atoms ( $\alpha$ , Figure 7) and the acyclic S(4) and S(7) ones ( $\beta$ ) are similar; benzene rings are essentially planar; in the pyrazine rings the N(1), N(2), C(24) and C(25) atoms lie in one plane, C(23) and C(26) deviate from it by (average) 0.09 and 0.07 Å (in opposite directions). The adjacent C–C bonds are inclined by 0–7.6° to the benzene and by 0.5–13.1° to the pyrazine ring planes (average 3.6 and 5.4°). Apparently, dithiole rings are (conformationally) the “weak links” in the macrocycle, being the easiest to fold.

Dimers with a usual ring-over-bond overlap exist both in **11a** (between inversion-related molecules) and in **11b** (between two crystallographically independent molecules). The contacting C<sub>2</sub>S<sub>4</sub> planes are strictly parallel in **11a** and insignificantly inclined in **11b** (4°), with an interplanar separation of 3.38 (**11a**) and 3.37 Å (**11b**). The shortest atom–atom contacts are C(1)⋯C(1') 3.42 Å in **11a**, C(1A)⋯C(4B) 3.38 Å in **11b**. Such distances are common for other TTF dimers<sup>[39]</sup> and longer than in some unbridged ones, for example, benzoylthio-triMe-TTF (interplanar separation 3.33 Å).<sup>[39c]</sup>

Molecule **20** (Figure 10, Table 2) lies on a mirror plane, passing through the midpoints of the C(1)–C(1'), C(6)–C(6') and C(8)–C(8') bonds. The “total” TTF bending ( $\theta + \phi$ ) of 54.3° is comparable with the *larger* values in **22a–d** (52.1, 52.8, 54.0, 49.7°) and exceeds the *average* values in these molecules (48.6,

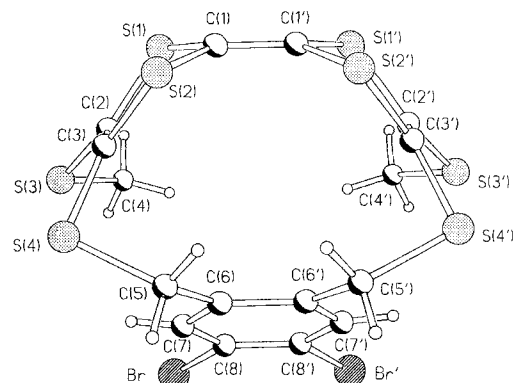
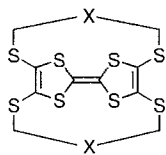


Figure 10. Molecular structure of **20**; atoms related via mirror plane are marked with primes.





- 22 a X =
- b X = CH<sub>2</sub>N(Me)CH<sub>2</sub>
- c X = CH<sub>2</sub>OCH<sub>2</sub>
- d X = CH<sub>2</sub>SCH<sub>2</sub>

48.2, 51.3 and 49.2°, respectively).<sup>[22b, d]</sup> Thus the bending effect of one six-membered bridge is marginally stronger than that of two seven-membered. Otherwise distortions of the macrocycle are small: the benzene ring is planar and the C(5)–C(6) bond is tilted by 4.5° out of its plane.

Unlike **11**, **20** does not form a dimer in the crystal. The TTF moiety forms intermolecular contacts S(1)⋯C(7) of 3.33 Å (with a benzene ring) on one edge and S(2)⋯Br of 3.62 Å on the other (cf. sum of the van der Waals radii, 3.65 and 3.80 Å),<sup>[42]</sup> while the π orbital of C(1) points towards the intramolecular cavity.

In both **11** and **20** the “outer” (*c*, Figure 7) C–S distances are longer than the “inner” (*b*) ones by 0.01–0.02 Å. Although the effect is marginal (1.5–4 e.s.d.), it is also observed in other strongly bent TTF derivatives.<sup>[21, 22]</sup> On the other hand, in (RS)<sub>4</sub>TTF molecules with long linear R groups, where the TTF system is planar,<sup>[12b, 43]</sup> *b* is equal to, or slightly (0.004–0.008 Å) longer than *c*, while in (planar) unsubstituted TTF, *b* – *c* = 0.025 Å.<sup>[34b, c]</sup> The comparison of planar<sup>[41]</sup> and bent<sup>[40]</sup> (MeS)<sub>4</sub>TTF (*b* – *c* = –0.003 and –0.014 Å, respectively) shows the same trend (cf. the individual C–S distances show an e.s.d. of ca. 0.002 Å). The effect can be attributed to the localisation of the HOMO on the central C<sub>2</sub>S<sub>4</sub> moiety, which is enhanced both by bending and by the presence of thioalkyl substituents (see above).

In both **11** and **20** the “outer” (*c*, Figure 7) C–S distances are longer than the “inner” (*b*) ones by 0.01–0.02 Å. Although the effect is marginal (1.5–4 e.s.d.), it is also observed in other strongly bent TTF derivatives.<sup>[21, 22]</sup> On the other hand, in (RS)<sub>4</sub>TTF molecules with long linear R groups, where the TTF system is planar,<sup>[12b, 43]</sup> *b* is equal to, or slightly (0.004–0.008 Å) longer than *c*, while in (planar) unsubstituted TTF, *b* – *c* = 0.025 Å.<sup>[34b, c]</sup> The comparison of planar<sup>[41]</sup> and bent<sup>[40]</sup> (MeS)<sub>4</sub>TTF (*b* – *c* = –0.003 and –0.014 Å, respectively) shows the same trend (cf. the individual C–S distances show an e.s.d. of ca. 0.002 Å). The effect can be attributed to the localisation of the HOMO on the central C<sub>2</sub>S<sub>4</sub> moiety, which is enhanced both by bending and by the presence of thioalkyl substituents (see above).

## Conclusions

In summary, we have reported the synthesis of the first pyrazinoporphyrazine derivatives functionalised with TTF units, as well as some unusual TTF-containing macrocycles synthesised during the course of this work. The solution electrochemistry of these new molecules has been studied, and the X-ray crystal structures of two severely distorted TTF derivatives have been determined. This work extends the chemistry of TTF derivatives in two areas of current interest, namely, supramolecular chemistry and unusual macrocyclic structures. Further studies on related TTF macrocycles and phthalocyanine systems are in progress.

## Experimental Section

<sup>1</sup>H NMR spectra were recorded at room temperature on a Varian VXR-200 spectrometer operating at 200.14 MHz and chemical shifts are reported in ppm downfield of tetramethylsilane. IR spectra were obtained with a Perkin-Elmer PE 1615 FTIR spectrometer. UV/Vis spectra were recorded on a UNICAM UV2 spectrophotometer and data were processed by a Vision Scan V2.11 programme. Mass spectra (EI, CI) were recorded using a VG 7070 E instrument operating at 70 eV. Plasma desorption mass spectra (PDMS) were recorded on a BioIon 10K. MALDI TOF mass spectra were obtained on a Kratos IV instrument in the reflection mode, operating with irradiation from a nitrogen laser at 337 nm. The matrix was 2,5-dihydroxybenzoic acid and spectra were averaged over 100 pulses whilst scanning across the sample: peak half-widths were 6–10 amu. Melting points were determined with a

Reichert micro hot-stage apparatus and are uncorrected. Solution electrochemistry was performed with a BAS CV-50W Electrochemical Analyser; for the experimental details see Table 1. Dichloromethane and dimethylformamide used in electrochemistry and UV/Vis spectroscopy were dried over phosphorus pentoxide and distilled under argon prior to use. Molecular modelling studies were performed using the Discover 2.9.7/95.0/3.0.0 programme in the Insight II 95.0 package. All chemicals were purchased either from Aldrich or Fluka and were used directly without further purification unless otherwise indicated.

**4-Methylthio-5-benzoylthio-1,3-dithiole-2-thione (6):** To a solution of zincate salt **5**<sup>[44]</sup> (14.37 g, 20 mmol) in dry acetone (300 mL), benzoyl chloride (5.62 g, 40 mmol) was added in one portion under stirring at room temperature. The mixture was stirred for an additional 0.5 h, followed by the addition of methyl iodide (5 mL) in one portion. After another 2 h of stirring, the green mixture, which contained a red precipitate, was evaporated in vacuo. The residue was washed with a large amount of water, leaving a red oil, which was dissolved in dichloromethane/hexanes (1:1 v/v) and chromatographed on a silica gel column (eluent dichloromethane/hexanes (1:1 v/v)) to separate, in order of elution: bis(methylthio)-1,3-dithiole-2-thione, **6** and bis(benzoylthio)-1,3-dithiole-2-thione. Compound **6** eluted as an oil, which crystallised from acetone as yellow–orange plates (9.8 g, 78%). M.p. 72–73 °C; <sup>1</sup>H NMR (CDCl<sub>3</sub>): δ = 2.53 (s, 3 H), 7.5–8.0 (m, 5 H); MS: *m/z* (%) = 316 (6.38, EI) [*M*<sup>+</sup>]; 317 (100, CI) [*M*<sup>+</sup> + 1]. C<sub>11</sub>H<sub>8</sub>OS<sub>3</sub> calcd C, 41.74; H, 2.55; found C, 42.07 H, 2.51.

**4,4'-Dibromomethylbenzil (3):** 4,4'-Dimethylbenzil (10.8 g, 45 mmol), finely ground *N*-bromosuccinimide (17.0 g, 95.5 mmol) and benzoyl peroxide (0.1 g) were suspended in carbon tetrachloride (100 mL, HPLC grade). The mixture was warmed with stirring and irradiated under sunlight until the carbon tetrachloride started to reflux. The heater was removed and the mixture was continuously stirred under sunlight for 20 min, by which time a viscous yellow syrup was obtained. The mixture was filtered under vacuum and the filtrate was washed with methanol, yielding **3** as bright yellow microplates (12.6 g, 71%). M.p. 190–192 °C; <sup>1</sup>H NMR ([D<sub>6</sub>]DMSO): δ = 4.78 (s, 2H), 7.67 (d, *J* = 8.5 Hz, 2H), 7.92 (d, *J* = 8.5 Hz, 2H); IR (KBr):  $\tilde{\nu}$  = 1674.8 cm<sup>-1</sup> (C=O); C<sub>16</sub>H<sub>12</sub>Br<sub>2</sub>O<sub>2</sub>, calcd C, 48.48; H, 3.03; found C, 48.97; H 3.15.

**2,3-Bis(4-bromomethylphenyl)-5,6-dicyano-1,4-pyrazine (4):** A mixture of **3** (11.46 g, 29 mmol), diaminomaleonitrile (3.76 g, 34.8 mmol) and acetic acid (100 mL) was stirred under reflux for 4 h. After cooling to room temperature, the solvent was removed in vacuo leaving a brown oily residue, which was dissolved in methanol (50 mL). The precipitate which formed on cooling was collected to afford **4** as white prisms (9.05 g, 67%). M.p. 152–154 °C; <sup>1</sup>H NMR (CDCl<sub>3</sub>): δ = 4.49 (s, 2H), 7.41 (d, *J* = 8.2 Hz, 2H), 7.54 (d, *J* = 8.2 Hz, 2H); IR (KBr):  $\tilde{\nu}$  = 2235, 1607, 1509, 1379 cm<sup>-1</sup>; MS (DCI): *m/z* (%) = 468 (3.22) [*M*<sup>+</sup>], 486 (10.28) [*M*<sup>+</sup> + 18]; C<sub>20</sub>H<sub>12</sub>Br<sub>2</sub>N<sub>4</sub> calcd C, 51.28; H, 2.56; N, 11.97; found C, 51.73; H, 2.50; N, 12.09.

**2,3-Dicyano-5,6-bis{4-[4-(5-methylthio-2-thioxo-1,3-dithioly)thiomethyl]-phenyl}-1,4-pyrazine (7):** To a sodium methoxide solution (made from sodium metal (0.67 g, 29.1 mmol) and dry methanol (150 mL)) **6** (9.2 g, 29.1 mmol) was added in one portion. The mixture was warmed to ca. 40 °C and stirred until all the solid dissolved to form a red–orange solution, when **4** (6.8 g, 14.5 mmol) was added in one portion, and a yellow solid immediately formed. Stirring was maintained at 40 °C for 1 hr, then the precipitate was collected by filtration under vacuum. The precipitate was dissolved in dichloromethane and chromatographed on a silica column (eluent dichloromethane) to afford **7** as a deep yellow amorphous solid (5.56 g, 52%). M.p. from 65 °C; <sup>1</sup>H NMR (CDCl<sub>3</sub>): δ = 2.48 (s, 3H), 4.03 (s, 2H), 7.44 (q, 4H); IR (KBr):  $\tilde{\nu}$  = 2235, 1604, 1508, 1375, 1061 cm<sup>-1</sup>; MS (DCI): *m/z* (%) = 731 (1.88) [*M*<sup>+</sup> + 1]; HRMS: found 729.8913; C<sub>28</sub>H<sub>18</sub>N<sub>4</sub>S<sub>10</sub> requires 729.8907.

**2,3-Dicyano-5,6-bis{4-[4-(5-methylthio-2-oxo-1,3-dithioly)thiomethyl]-phenyl}-1,4-pyrazine (8):** Compound **7** (4.9 g, 6.7 mmol) was dissolved in a mixture of chloroform (100 mL) and acetic acid (33 mL). Mercury(II) acetate (11 g, 34.5 mmol) was added and the mixture was stirred at room temperature for 24 h. The light yellow milky suspension was then filtered under vacuum through Celite and the filter washed with chloroform (3 ×). The bright yellow filtrate was evaporated under vacuum to leave a yellow solid, which was redissolved in chloroform (50 mL). The solution was washed with cold satu-

rated sodium hydrogen carbonate solution until the aqueous phase was basic, then washed once more with water. The organic phase was separated, dried ( $\text{MgSO}_4$ ), and filtered through a short silica column to yield **8** as bright yellow amorphous solid (3.8 g, 80%). M.p. from 52 °C;  $^1\text{H NMR}$  ( $\text{CDCl}_3$ ):  $\delta$  = 2.41 (s, 3H), 4.02 (s, 2H), 7.31 (d,  $J$  = 8.4 Hz, 2H), 7.51 (d,  $J$  = 8.4 Hz, 2H); IR (KBr):  $\tilde{\nu}$  = 2235, 1664, 1609, 1375  $\text{cm}^{-1}$ ; MS:  $m/z$  (%) = 698 (6.06, EI) [ $M^+$ ], 716 (9.06, DCI) [ $M^+ + 18$ ];  $\text{C}_{28}\text{H}_{18}\text{N}_4\text{O}_2\text{S}_8$  calcd C, 48.11; H, 2.60; N, 8.02; found C, 47.85; H, 2.46; N, 7.86.

**Cross-Coupling of 8 and 9—Synthesis of 10 and 11:** A mixture of **8** (0.73 g, 1.04 mmol) and **9**<sup>[15]</sup> (1.10 g, 3 mmol) in triethyl phosphite (10 mL) under argon was stirred and heated (oil bath temperature 115 °C) for 4 h. After cooling, evaporation under vacuum afforded a red oil to which methanol (20 mL) was added. The solvent was removed by decantation and the red oily residue obtained was chromatographed on a silica gel column (dichloromethane:hexanes (1:1 v/v)) affording (in the order of elution) **12** (0.18 g, 9% based on **9**), **10** (0.48 g, 35% based on **8**) and **11** (0.17 g, 24.6% based on **8**). Compound **10** is a light-brown mobile solid, attempted crystallisation of which proved unsuccessful.  $^1\text{H NMR}$  ( $\text{CDCl}_3$ ):  $\delta$  = 0.88 (m, 6H), 1.27 (m, 12H), 1.59 (m, 4H), 2.32 (s, 3H), 2.80 (sextet,  $J$  = 4.1 Hz, 4H), 3.98 (s, 2H), 7.31 (d,  $J$  = 8.2 Hz, 2H), 7.53 (d,  $J$  = 8.2 Hz); IR (KBr):  $\tilde{\nu}$  = 2923, 2240, 1605, 1508, 1375  $\text{cm}^{-1}$ ; PDMS:  $m/z$  = 1334 [ $M^+$ ]. Compound **11** was crystallised from either carbon disulfide or dichloromethane, giving red prisms suitable for X-ray structural analysis. M.p. > 250 °C;  $^1\text{H NMR}$  ( $\text{CDCl}_3$ ):  $\delta$  = 2.06 (s, 6H), 3.80 (d,  $J$  = 13.5 Hz, 2H), 4.21 (d,  $J$  = 13.5 Hz, 2H), 7.42 (d,  $J$  = 8.3 Hz, 2H), 7.52 (d,  $J$  = 8.3 Hz, 2H); HRMS: found 665.92792;  $\text{C}_{28}\text{H}_{18}\text{N}_4\text{S}_8$  requires 665.92972.

**Synthesis of 11 by self-coupling of 8:** A mixture of **8** (160 mg) and triethyl phosphite (10 mL) was stirred and heated in an oil bath at 115 °C under argon for 3 h. On cooling, the solvent was removed in vacuo, leaving an oily red residue. Methanol (10 mL) was added and the solid that precipitated was collected by suction and washed with a large amount of methanol. The solid was dissolved in dichloromethane and purified by column chromatography (silica gel, dichloromethane) to give pure **10** (77.1 mg, 51%).

**Pyrazinoporphyrazines 13a–c:** To a solution of **10** (140 mg for **13a**, 145 mg for **13b**, 198 mg for **13c**) in 1,4-dioxane (2 mL)<sup>[7]</sup> (freshly distilled from sodium/benzophenone) freshly prepared lithium pentoxide solution in amyl alcohol (1.89 M, 5 mL) was added. The mixture was immersed in an oil bath at 125 °C and stirred for 45 min under argon. The mixture was then cooled to room temperature and absolute ethanol (30 mL) was added. The mixture was left to stand overnight. The green precipitate was collected by decanting the solvent, filtration under vacuum, and then washed with a large amount of absolute ethanol. The precipitate was dissolved in chloroform (2 mL) to give a dark-green solution to which acetic acid (1 mL) for **13a** or the corresponding metal salt (4 equiv, zinc acetate for **13b**, copper(II) chloride for **13c**) in absolute ethanol (30 mL) was added; the mixture was refluxed for 5 h. After cooling to room temperature the dark-green solid that precipitated was collected by vacuum filtration. The solid was extracted by boiling three times in absolute ethanol (30 mL) until the ethanol solution was colourless. The solid was then dissolved in either carbon disulfide or dichloromethane and filtered through a Celite column to remove any inorganic impurities that may have been present. Concentration of the filtrate afforded **13a–c** as a dark-green solid. **13a**: 89 mg (64%); M.p. ca. 80 °C; UV/Vis (1:1, v/v, *o*-dichlorobenzene/acetic acid):  $\lambda_{\text{max}}$  (log $\epsilon$ ) = 676.5 (4.47), 654.0 (4.40) nm; MALDI-TOF MS:  $m/z$  = 5320;  $\text{C}_{232}\text{H}_{282}\text{N}_{16}\text{S}_{64}$  requires 5346; calcd C, 52.12; H, 5.32; N, 4.19; found C, 51.97, H, 5.49; N, 3.95. **13b**: (66 mg, 45%). M.p. > 250 °C; UV/Vis (DCM):  $\lambda_{\text{max}}$  (log $\epsilon$ ) = 664 (4.53) nm; MALDI-TOF MS:  $m/z$  = 5420;  $\text{C}_{232}\text{H}_{280}\text{N}_{16}\text{S}_{64}\text{Zn}$  requires 5409; calcd C, 51.50; H, 5.22; N, 4.14; found C, 50.82; H, 5.21; N, 3.90. **13c**: (63 mg, 31%); M.p. > 250 °C; UV/Vis (DCM):  $\lambda_{\text{max}}$  (log $\epsilon$ ) = 659 (4.84) nm; MALDI-TOF MS:  $m/z$  = 5450;  $\text{C}_{232}\text{H}_{280}\text{N}_{16}\text{S}_{64}\text{Cu}$  requires 5407; calcd C, 51.52; H, 5.21; N, 4.14; found C, 49.65; H, 5.14; N, 3.74.

**2,3-Bis(bromomethyl)-5,6-dicyano-1,4-pyrazine (14):** A mixture of  $\alpha,\alpha'$ -dibromodiacyetyl<sup>[45]</sup> (6.1 g, 25 mmol), diaminomaleonitrile (2.7 g, 25 mmol) and ethanol (50 mL)<sup>[46]</sup> was refluxed for 3 h to obtain a brown solution. The solvent was removed in vacuo and the residue chromatographed on a silica column (eluent dichloromethane). The first product to elute was compound **14** as a colourless oil, which crystallised from methanol as white prisms (6.2 g, 78%). M.p. 106–107 °C;  $^1\text{H NMR}$  ( $\text{CDCl}_3$ ):  $\delta$  = 4.75(s);  $m/z$  (%) = 316

(7.5) [ $M^+$ ].  $\text{C}_8\text{H}_4\text{Br}_2\text{N}_4$  calcd C, 30.41; H, 1.28; N, 17.73; found C, 30.54; H, 1.17; N, 17.76. A second product, which eluted after **14**, was a colourless oil identified as 2,3-dicyano-5,6-di(ethoxymethyl)-1,4-pyrazine by  $^1\text{H NMR}$  spectroscopy:  $^1\text{H NMR}$  ( $\text{CDCl}_3$ ):  $\delta$  = 1.27 (6H, t,  $J$  = 7.0 Hz), 3.64 (4H, q,  $J$  = 7.0 Hz), 4.84 (4H, s).

**2,3-Dicyano-5,6-bis[4-(5-methylthio-2-thione-1,3-dithioly)thiomethyl]-1,4-pyrazine (15):** To sodium methoxide solution (prepared from sodium (0.50 g, 21.7 mmol) and dry methanol (200 mL)) at room temperature, compound **6** (6.88 g, 21.7 mmole) was added in one portion and the mixture was stirred and warmed to ca. 40 °C to afford a red-orange solution. Compound **14** (3.43 g, 10.8 mmol) was added to the stirred solution, which was then refluxed for 0.5 h. The reaction mixture was cooled to room temperature and the precipitate was filtered in vacuo and washed sequentially with a large volume of water and methanol, to give a red-orange solid (5.6 g, 90%), which was recrystallised from hot benzonitrile to afford **15** as pale brown prisms. M.p. 151–153 °C;  $^1\text{H NMR}$  ( $\text{CDCl}_3$ ):  $\delta$  = 2.49 (s, 3H), 4.32 (s, 2H).  $\text{C}_{16}\text{H}_{10}\text{N}_4\text{S}_{10}$ : calcd C, 33.19; H, 1.74; N, 9.68; found C, 33.48; H, 1.67; N, 9.58.

**Compound 17:** Compound **16**<sup>[23]</sup> (2.43 g, 4.0 mmol) was dissolved in degassed DMF (60 mL) and a solution of  $\text{CsOH} \cdot \text{H}_2\text{O}$  (0.71 g, 4.2 mmol) in methanol (10 mL) was added dropwise and the mixture was stirred at room temperature overnight to yield a red solution. Compound **14** (0.65 g, 2.06 mmol) was added in one portion and stirring was maintained for 1.5 h. Solvent was removed in vacuo to leave a brown residue, which was chromatographed on a silica column (eluent DCM/light petroleum, b.p. 40–60 °C (2:1 v/v)) to afford **17** as an amorphous brown solid (2.0 g, 79%) M.p. from 52 °C;  $^1\text{H NMR}$  ( $\text{CDCl}_3$ ):  $\delta$  = 7.13 (s, 16H), 4.27 (s, 4H), 3.87 (s, 4H), 3.85 (s, 4H), 2.39 (s, 6H) and 2.31 (s, 12H).  $\text{C}_{34}\text{H}_{46}\text{N}_4\text{S}_{16}$ : calcd C, 51.31; H, 3.67; N, 4.43; found C, 51.36; H, 3.51; N, 4.28.

**1,2-Dibromo-3,4-bis[4-(5-methylthio-2-thione-1,3-dithioly)thiomethyl] benzene (18):** To the sodium thiolate solution prepared from **6** (5.06 g, 16 mmol) and sodium methoxide (16.1 mmol) in dry methanol (150 mL), 1,2-dibromo-4,5-bis(bromomethyl) benzene<sup>[47]</sup> (3.37 g, 8 mmol) was added in one portion. The mixture was vigorously stirred at room temperature for 1 h, then warmed to 50 °C with stirring for an additional 20 min. Water (100 mL) was added to the mixture followed by cooling with ice. The resulting yellow solid was isolated by decanting the solvent, vacuum filtration, and crystallisation from dichloromethane to give **18** as yellow flakes (4.5 g, 82%). A yellow prism suitable for X-ray structural analysis was obtained by recrystallisation from carbon disulfide. M.p. 177–178.5 °C;  $^1\text{H NMR}$  ( $\text{CDCl}_3$ ):  $\delta$  = 2.46 (s, 6H), 4.11 (s, 4H), 7.49 (s, 2H).  $\text{C}_{16}\text{H}_{12}\text{Br}_2\text{S}_{10}$ : calcd C, 28.07; H, 1.77; found C, 27.43; H, 1.75.

**1,2-Dibromo-3,4-bis[4-(5-methylthio-2-oxo-1,3-dithioly)thiomethyl] benzene (19):** By a similar procedure to the transformation of **7** to **8**, **19** was obtained by transchalcogenation of **18** (3.87 g, 5.65 mmol), in chloroform (300 mL) and acetic acid (100 mL) with mercury(II) acetate (8.9 g, 28.3 mmol) The product was crystallised from carbon disulfide forming **19** as light yellow needles (3.3 g, 89%). M.p. 131–133 °C.  $^1\text{H NMR}$  ( $\text{CDCl}_3$ ):  $\delta$  = 2.39 (s, 6H), 4.10 (s, 4H), 7.47 (s, 2H);  $\text{C}_{16}\text{H}_{12}\text{Br}_2\text{O}_2\text{S}_8$  calcd C, 29.45; H, 1.85; found C, 28.90; H, 1.96.

**Self-Coupling of 19—Synthesis of 20 and 21:** Compound **19** (0.65 g, 1 mmol) was mixed with degassed triethyl phosphite (20 mL) and the mixture was heated with stirring under argon at an oil bath temperature of 125 °C, forming a yellow solution. An orange precipitate gradually appeared and the mixture was stirred with heating for 2 h. Triethyl phosphite was removed in vacuo, and ethanol (20 mL) was added to the residue. The solid was collected by filtration in vacuo and washed with a large amount of ethanol, yielding a dark yellow powder (0.55 g), which was a mixture of **20** and **21**. Due to the very limited solubility of this mixture in usual organic solvents, column chromatography was not possible. Nevertheless, repeated extraction with hot carbon disulfide left the less soluble white needles, which were shown to be **20** by X-ray crystallography, m.p. ca. 210 °C (after darkening at > 150 °C). (The crystal of **20** for X-ray analysis was grown as follows: the sample (ca. 5 mg) was mixed with carbon disulfide (ca. 0.5 mL), placed in a sealed glass tube, and heated above the boiling point of the solvent until dissolution was complete. Cooling the sample yielded a mixture of white needles of **20** and an orange powder of **21**.) The product obtained by evaporation of the  $\text{CS}_2$

Table 3. Crystal data.

Compound	11a	11b	15	18	20
formula	C <sub>28</sub> H <sub>18</sub> N <sub>4</sub> S <sub>8</sub> ·CS <sub>2</sub>	C <sub>28</sub> H <sub>18</sub> N <sub>4</sub> S <sub>8</sub> ·CH <sub>2</sub> Cl <sub>2</sub>	C <sub>16</sub> H <sub>10</sub> N <sub>2</sub> S <sub>10</sub>	C <sub>16</sub> H <sub>12</sub> Br <sub>2</sub> S <sub>10</sub>	C <sub>16</sub> H <sub>12</sub> Br <sub>2</sub> S <sub>8</sub>
M <sub>r</sub>	743.07	751.87	578.88	684.68	620.56
T, K	150	150	150	150	296
symmetry	monoclinic	triclinic	triclinic	monoclinic	monoclinic
a, Å	8.052(3)	11.408(1)	9.054(1)	11.850(1)	8.209(1)
b, Å	21.305(3)	16.057(1)	9.248(1)	12.056(1)	16.124(2)
c, Å	19.941(3)	19.819(1)	15.283(2)	16.511(1)	8.418(2)
α, °	90	94.78(1)	96.32(1)	90	90
β, °	100.32(2)	106.58(1)	100.22(1)	97.53(1)	98.97(1)
γ, °	90	102.05(1)	107.73(1)	90	90
U, Å <sup>3</sup>	3365.5(14)	3363.0(4)	1181.0(2)	2338.4(6)	1100.6(3)
space group	P2 <sub>1</sub> /c (no. 14)	P $\bar{1}$ (no. 2)	P $\bar{1}$ (no. 2)	P2 <sub>1</sub> /n (no. 14)	Im (no. 8)
Z	4	4	2	4	2
F(000)	1520	1536	588	1352	612
μ, cm <sup>-1</sup>	63.0	7.2	9.5	43.6	44.4
ρ <sub>calc</sub> , g cm <sup>-3</sup>	1.47	1.485	1.628	1.945	1.87
crystal size, mm	0.1 × 0.1 × 0.25	0.04 × 0.38 × 0.40	0.14 × 0.16 × 0.22	0.25 × 0.4 × 0.55	0.05 × 0.1 × 0.2
2θ <sub>max</sub> , °	120	56	51.2	52	51.4
data total	5078	20327	5292	9890	2590
data unique	4677	11768	3755	4064	1279
data observed, I > 2σ(I)	3116	9360	3203	3727	1175
R <sub>int</sub> [a]	-/0.043	0.041/0.033	0.035/0.026	0.123/0.041	0.054/0.035
absorption correction	empirical [b]	integration [c]	semiempirical [c,d]	integration [c]	semiempirical [c,d]
transmission, min:max	0.73:1.00	0.76:0.97	0.77:0.91	0.18:0.38	0.79:0.99
no. of variables	398	833	311	302	133
wR(F <sup>2</sup> ), all data	0.108	0.172	0.098	0.083	0.073
goodness-of-fit	1.03	1.03	1.109	1.10	1.10
R(F), obs. data	0.055	0.053	0.035	0.033	0.030
Δρ <sub>max/min</sub> , e Å <sup>-3</sup>	0.41/ - 0.35	0.52/ - 1.34	0.35/ - 0.32	0.37/ - 0.51	0.38/ - 0.35

[a] Before and after absorption correction. [b] 36 ψ scans of 1 reflection, TEXSAN software [49]. [c] SHELXTL software. [d] On Laue equivalents.

solution was dissolved in *o*-dichlorobenzene to which dichloromethane was added to afford **21** as an orange powder, m.p. > 250 °C. C<sub>32</sub>H<sub>24</sub>Br<sub>4</sub>S<sub>16</sub>: calcd C, 30.97; H, 1.95; found C, 31.08; H, 1.87. By the very different methylene proton NMR signals in CDCl<sub>3</sub> (**20**, 4.18 (d, 2H, *J* = 16 Hz), 3.47 (d, 2H, *J* = 16 Hz); **21**, 4.09 (s, 4H)), the relative ratio of **20**:**21** in the part of the crude product mixture that dissolved in CDCl<sub>3</sub> was ca. 2:1. Both **20** and **21** showed additional peaks at 2.24 (s, 6H) and 8.18 (s, 2H).

**Crystal Structure Analysis:** Single-crystal X-ray diffraction experiments were carried out on a Siemens 3-circle diffractometer with a CCD area detector (MoK $\alpha$  radiation,  $\lambda$  = 0.71073 Å,  $\omega$  scan mode with 0.3° steps), for **11a** on a 4-circle Rigaku AFC6S diffractometer (CuK $\alpha$  radiation,  $\lambda$  = 1.54084 Å,  $\omega$  scan mode with Lehmann-Larsen algorithm), using graphite monochromators and Cryostream open-flow N<sub>2</sub> gas cryostats. The structures were solved by direct methods (**18** by Patterson technique) and refined by full-matrix least squares against F<sup>2</sup> of all data, using SHELXTL software.<sup>[48]</sup> All non-H atoms were refined with anisotropic displacement parameters. H atoms in **11a** and **11b** were treated as "riding", in **15** and **18** refined isotropically; in **20** the methyl group was refined as a rigid body, other H atoms isotropically. In **11a**, the C(9)H<sub>3</sub> methyl group of **11** and the S(10) atom of crystallisation CS<sub>2</sub> are disordered each over two positions, A and B, with occupancies of 0.6 and 0.4, respectively. In **11b**, one of the CH<sub>2</sub>Cl<sub>2</sub> molecules shows a complicated disorder, approximated as atoms Cl(3) and Cl(4) occupying two positions (A and B) each, with occupancies of 0.5, and the carbon atom C(02) in three positions, A, B, and C, with occupancies of 0.7, 0.2, and 0.1, respectively. The crystal of **20** was a racemic twin; the contributions of the components were refined to 82(2) and 18(2)%. Crystal data and experimental details are listed in Table 3.

Crystallographic data (excluding structure factors) for the structures reported in this paper have been deposited with the Cambridge Crystallographic Data Centre as supplementary publication no. CCDC-1220-52. Copies of the data can be obtained free of charge on application to The Director, CCDC, 12 Union Road, Cambridge CB21EZ, UK (Fax: Int. code +(1223)336-0333; e-mail: deposit@chemcryst.cam.ac.uk).

**Acknowledgement:** This work was funded by the EPSRC.

Received: February 13, 1997 [F 609]

- Reviews: a) C. C. Leznoff, A. B. P. Lever (Eds) *Phthalocyanines, Properties and Applications*, Vols. 1-3, VCH, New York, 1989–1993; b) H. Schultz, H. Lehmann, M. Rein, M. Hanack, *Struct. Bonding* (Berlin) **1990**, *74*, 41; c) M. Hanack, M. Lang, *Adv. Mater.* **1994**, *6*, 819.
- Review: C. C. Leznoff in ref. [1a], **1989**, *Vol. 1*, 1.
- D. Lelievre, O. Damette, J. Simon, *J. Chem. Soc. Chem. Commun.* **1993**, 939.
- a) F. Fernandez-Lazaro, A. Sastre, T. Torres, *J. Chem. Soc. Chem. Commun.* **1994**, 1525; b) N. Kobayashi, Y. Higashi, T. Osa, *ibid.* **1994**, 1785; c) P. J. Brach, S. J. Grammatica, O. A. Ossanna, L. Weinberger, *J. Heterocycl. Chem.* **1970**, *7*, 1403; d) B. Mohr, G. Wegner, K. Ohta, *J. Chem. Soc. Chem. Commun.* **1995**, 995; e) M. J. Cook, A. Jafari-Fini, *J. Mater. Chem.* **1997**, *7*, 5.
- C. S. Velazquez, T. F. Baumann, M. M. Olmstead, H. Hope, A. G. M. Barrett, B. M. Hoffman, *J. Am. Chem. Soc.* **1993**, *115*, 9997.
- T. G. Linssen, K. Dürr, M. Hanack, A. Hirsch, *J. Chem. Soc. Chem. Commun.* **1995**, 103.
- R. D. George, A. W. Snow, *Chem. Mater.* **1994**, *6*, 1587.
- a) C. F. van Nostrum, S. J. Picken, R. J. M. Nolte, *Angew. Chem. Int. Ed. Engl.* **1994**, *33*, 2173; b) C. F. van Nostrum, R. J. M. Nolte, *Chem. Commun.* **1996**, 2385.
- M. J. Cook, G. Cooke, A. Jafari-Fini, *J. Chem. Soc. Chem. Commun.* **1995**, 1715.
- F. Wudl, D. Wobschall, E. J. Hufnagel, *J. Am. Chem. Soc.* **1972**, *94*, 671;
- a) J. R. Ferraro, J. M. Williams, *Introduction to Synthetic Electrical Conductors*, Academic Press, London, **1987**; b) M. R. Bryce, *Chem. Soc. Rev.* **1991**, *20*, 355; c) *J. Mater. Chem.* **1995**, *5*, 1469–1753 (Special Issue on Molecular Conductors).
- a) T. Jørgensen, T. K. Hansen, J. Becher, *Chem. Soc. Rev.* **1994**, *23*, 41; b) A. S. Batsanov, N. Svenstrup, J. Lau, J. Becher, M. R. Bryce, J. A. K. Howard, *J. Chem. Soc. Chem. Commun.* **1995**, 1201; c) P. Blanchard, N. Svenstrup, J. Becher, *ibid.* **1996**, 615; d) Z. T. Li, P. C. Stein, N. Svenstrup, K. H. Lund, J. Becher, *Angew. Chem. Int. Ed. Engl.* **1996**, *34*, 2524.
- a) M. A. Blower, M. R. Bryce, W. Devonport, *Adv. Mater.* **1996**, *8*, 63; b) M. A. Blower, M. R. Bryce, unpublished results.
- P. Wu, G. Saito, K. Imaeda, Z. Shi, T. Mori, T. Enoki, H. Inokuchi, *Chem. Lett.* **1986**, 441.
- For an alternative route to a mono-protected 1,3-dithiole-2-thione see: J. Becher, J. Lau, P. Leriche, P. Mork, N. Svenstrup, *J. Chem. Soc. Chem. Commun.* **1994**, 2715.
- When the bridging groups between two bis(1,3-dithiole-2-thiones) (ones) are sufficiently short (or rigid) tetrathiafulvalenophanes can be formed by intermolecular phosphite coupling: a) K. Matsuo, K. Takimiya, Y. Aso, T. Otsubo and F. Ogura, *Chem. Lett.* **1995**, 523; b) K. Takimiya, Y. Aso, F. Ogura, T. Otsubo, *Chem. Lett.* **1995**, 753.

- [17] The use of dioxane as a co-solvent in phthalonitrile tetramerisation was suggested in a personal communication from Prof. E. H. Mørkved, NTH, Norway.
- [18] a) S. Hünig, G. Kiesslich, H. Quast, D. Scheutzow, *Liebigs Ann. Chem.* **1973**, 310; b) J. B. Torrance, B. A. Scott, B. Welber, F. B. Kaufman, P. E. Seiden, *Phys. Rev. B* **1979**, 19, 730.
- [19] F. Vögtle, *Fascinating Molecules in Organic Chemistry*, Wiley, Chichester, **1992**, 271.
- [20] C. S. Wang, C. F. Stanley, M. R. Bryce, A. Beeby, A. S. Batsanov, J. A. K. Howard, *J. Chem. Soc. Perkin Trans. 2*, in press.
- [21] Review: T. Otsubo, Y. Aso, K. Takimiya, *Adv. Mater.* **1996**, 8, 203
- [22] Leading references: a) J. Röhrich, P. Wolf, V. Enkelmann, K. Müllen, *Angew. Chem. Int. Ed. Engl.* **1988**, 27, 1377; b) T. Jørgensen, B. Girmay, T. K. Hansen, J. Becher, A. E. Underhill, M. B. Hursthouse, M. E. Harman, J. D. Kilburn, *J. Chem. Soc. Perkin Trans. 1*, **1992**, 2907; c) M. Adam, V. Enkelmann, H.-J. Räder, J. Röhrich, K. Müllen, *Angew. Chem. Int. Ed. Engl.* **1992**, 31, 309; d) T. K. Hansen, T. Jørgensen, F. Jensen, P. H. Thygesen, K. Christiansen, M. B. Hursthouse, M. E. Harman, M. A. Malik, B. Girmay, A. E. Underhill, M. Begtrup, J. D. Kilburn, K. Belmore, P. Roepstorff, J. Becher, *J. Org. Chem.* **1993**, 58, 1359; e) K. Boubekeur, C. Lenoir, P. Batail, R. Carlier, A. Tallec, M.-P. Le Paillard, D. Lorcy, A. Robert, *Angew. Chem. Int. Ed. Engl.* **1994**, 33, 1379; f) K. Boubekeur, P. Batail, F. Bertho, A. Robert, *Acta Crystallogr. Sect. C* **1991**, 47, 1109; g) H. A. Staab, J. Ippen, T. Chu, C. Krieger, B. Starker, *Angew. Chem. Int. Ed. Engl.* **1980**, 19, 66.
- [23] C. S. Wang, M. R. Bryce, A. S. Batsanov, L. M. Goldenberg, J. A. K. Howard, *J. Mater. Chem.* **1997**, 7, 1189.
- [24] D. L. Lichtenberger, R. L. Johnston, K. Hinkelmann, T. Suzuki, F. Wudl, *J. Am. Chem. Soc.* **1990**, 112, 3302.
- [25] a) M. Mizuno, A. F. Garito, M. P. Cava, *J. Chem. Soc. Chem. Commun.* **1978**, 18; b) A. J. Moore, M. R. Bryce, *ibid.* **1991**, 1638.
- [26] a) Review: M. Adam, K. Müllen, *Adv. Mater.*, **1994**, 6, 439; b) M. Jørgensen, K. A. Lerstrup, K. Bechgaard, *J. Org. Chem.* **1991**, 56, 5684; c) M. R. Bryce, G. J. Marshall, A. J. Moore, *ibid.* **1992**, 57, 4859.
- [27] a) M. R. Bryce, G. Cooke, A. S. Dhindsa, D. J. Ando, M. B. Hursthouse, *Tetrahedron Lett.* **1992**, 33, 1783; b) J. D. Martin, E. Canadell, J. Y. Becker, J. Bernstein, *Chem. Mater.* **1993**, 5, 1199; c) M. Fourmigué, Y.-S. Huang, *Organometallics* **1993**, 12, 797.
- [28] J. Y. Becker, J. Bernstein, A. Ellern, H. Gershtenman, V. Khodorkovsky, *J. Mater. Chem.* **1995**, 5, 1557.
- [29] For a review of redox-active dendrimers and hyper-branched systems see: M. R. Bryce, W. Devonport, *Advances in Dendritic Macromolecules*, Ed. G. Newkome, JAI Press, London, Vol. 3, **1996**, 115. For a discussion of the diffusion rates of molecules on the cyclic voltammetric time-scale see: D. Astruc, *Electron Transfer and Radical Processes in Transition Metal Chemistry*, VCH, New York, **1995**. Chapter 2. Thin-layer cyclic voltammetric techniques (which eliminate diffusion phenomena) have recently been applied for the first time to dendrimers: for a system containing 13 TTF units it was clear that all the TTF units are involved in the redox process (see ref. [23]). Cf. M. R. Bryce, W. Devonport, A. J. Moore, *Angew. Chem. Int. Ed. Engl.* **1994**, 33, 1761.
- [30] a) J.-L. Fillaut, J. Linaers, D. Astruc, *Angew. Chem. Int. Ed. Engl.* **1994**, 33, 2460; b) S. Campagne, G. Denti, S. Serroni, A. Juris, M. Venturi, V. Ricavuto, V. Balzani, *Chem. Eur. J.* **1995**, 1, 211; c) P. Jutz, C. Batz, B. Neumann, H.-G. Stammer, *Angew. Chem. Int. Ed. Engl.* **1996**, 35, 2118.
- [31] A. B. P. Lever, E. R. Milaeva, G. Speier in ref. [1 a], **1993**, Vol. 3, 1.
- [32] We note that molecular dynamics simulations of the interactions of segments of poly( $\gamma$ -benzyl glutamate) in solution suggest that the preferred conformation of macromolecules can be very solvent dependent: J. Helfrich, R. Hentschke, *Macromolecules* **1995**, 28, 3831.
- [33] P. J. Dandliker, F. Diederich, M. Gross, C. R. Knobler, A. Louati, E. M. Sanford, *Angew. Chem. Int. Ed. Engl.* **1994**, 33, 1739.
- [34] a) J. M. Williams, H. H. Wang, T. J. Emge, U. Geiser, M. A. Beno, P. C. W. Leung, K. D. Carlson, R. J. Thorn, A. J. Schultz, *Prog. Inorg. Chem.* **1987**, 35, 51 (review); b) W. F. Cooper, N. C. Kenny, J. W. Edmonds, A. Nagel, F. Wudl, P. Coppens, *J. Chem. Soc. Chem. Commun.* **1971**, 869; c) A. Ellern, J. Bernstein, J. Y. Becker, S. Zamir, L. Shahal, S. Cohen, *Chem. Mater.* **1994**, 6, 1378; d) J. P. Lowe, *J. Am. Chem. Soc.* **1980**, 102, 1262; e) B. D. Silverman, *J. Chem. Phys.* **1980**, 72, 5501.
- [35] I. Hargittai, J. Brunvoll, M. Kolonits, V. Khodorkovsky, *J. Mol. Struct.* **1994**, 317, 273.
- [36] Cambridge Structural Database, Version October **1996** release: F. H. Allen, J. E. Davies, J. J. Galloy, O. Johnson, O. Kennard, C. F. Macrae, E. M. Mitchell, G. F. Mitchell, J. M. Smith, D. G. Watson, *J. Chem. Info. Comput. Sci.* **1991**, 31, 187. The atomic coordinates of five most interesting macrocyclic structures (including **22c**),<sup>[22d-e]</sup> have not been published or deposited.
- [37] A. Izuoka, T. Tachikawa, T. Sugawara, Y. Suzuki, M. Konno, Y. Saito, H. Shinohara, *J. Chem. Soc. Chem. Commun.* **1992**, 1472.
- [38] a) C. Wang, A. Ellern, J. Y. Becker, J. Bernstein, *Tetrahedron Lett.* **1994**, 35, 8489; b) C. Wang, A. Ellern, V. Khodorkovsky, J. Y. Becker, J. Bernstein, *J. Chem. Soc. Chem. Commun.* **1994**, 2115.
- [39] a) A. S. Batsanov, M. R. Bryce, G. Cooke, A. S. Dhindsa, J. N. Heaton, J. A. K. Howard, A. J. Moore, M. C. Petty, *Chem. Mater.* **1994**, 6, 1419; b) A. S. Batsanov, M. R. Bryce, J. N. Heaton, A. J. Moore, P. J. Skabara, J. A. K. Howard, E. Ortí, P. M. Viruela, R. Viruela, *J. Mater. Chem.* **1995**, 5, 1689; c) A. J. Moore, M. R. Bryce, A. S. Batsanov, J. C. Cole, J. A. K. Howard, *Synthesis* **1995**, 675.
- [40] C. Katayama, M. Honda, H. Kumagai, J. Tanaka, G. Saito, H. Inokuchi, *Bull. Chem. Soc. Japan* **1985**, 58, 2272.
- [41] H. Endres, *Z. Naturforsch.* **1986**, 41B, 1351.
- [42] L. Pauling, *The Nature of the Chemical Bond*, 3rd Ed., Cornell University Press, Ithaca, **1960**. From: Yu. V. Zefirov, P. M. Zorkii, *Russ. Chem. Rev.* **1989**, 58, 421, slightly different values, C—Br 3.68; S—Br 3.81 Å.
- [43] a) C. Nakano, K. Imaeda, T. Mori, Y. Maruyama, H. Inokuchi, N. Iwasawa, G. Saito, *J. Mater. Chem.* **1991**, 1, 37; b) C. Nakano, T. Mori, K. Imaeda, N. Yasuoka, Y. Maruyama, H. Inokuchi, N. Iwasawa, G. Saito, *Bull. Chem. Soc. Japan* **1992**, 65, 1878; c) *ibid.* **1992**, 65, 2086.
- [44] a) G. Steimecke, H.-J. Sieler, R. Kirmse, E. Hoyer, *Phosphorus and Sulfur* **1979**, 7, 49; b) Review: N. Svenstrup, J. Becher, *Synthesis* **1995**, 215.
- [45] P. Ruggli, M. Herzog, J. Wegmann, H. Dahn, *Helv. Chim. Acta* **1946**, 29, 95.
- [46] Independently, the same reaction in acetonitrile gave **14** in almost quantitative yield: Prof. E. H. Mørkved, NTH, Norway, personal communication.
- [47] G. Pawlowski, M. Hanack, *Synthesis* **1980**, 287.
- [48] G. M. Sheldrick, SHELXTL, Version 5/VMS, **1995**, Siemens Analytical X-Ray Instruments Inc., Madison, WI, USA.
- [49] Molecular Structure Corporation, TEXSAN, TEXRAY Structure Analysis Package, Version 5, **1989**, MSC, The Woodlands, TX 77381, USA.